Atoms-in-molecules analysis of the effect of intermolecular interactions on dielectric properties in hydrogen-bonded material 5-bromo-9-hydroxyphenalenone

AUTHOR(S):

Otaki, Hiroki; Ando, Koji

Atoms-in-molecules analysis of the effect of intermolecular interactions on dielectric properties in hydrogen-bonded material 5-bromo-9-hydroxyphenalenone

Hiroki Otaki*, Koji Ando*

January 26, 2012

Abstract

Intermolecular interactions in molecular crystal of 5-bromo-9-hydroxyphenalenone are analyzed by means of Bader's theory of "Atoms in Molecules" (AIM). A set of criteria to ascertain the presence of a hydrogen bond is applied to two candidates of intermolecular contacts suggested by our previous work [Otaki, H.; Ando, K. *Phys. Chem. Chem. Phys.* **2011**, 13, 10719-10728]. It is shown that they almost satisfy the criteria to confirm the existence of intermolecular $C-H\cdots O$ hydrogen bond. In addition to the hydrogen bonding, other types of interactions, such as $H\cdots H$ and $H\cdots Br$, are found in one of the candidates. The discussions are extended to explain how the molecular dipole moment is induced by surrounding molecules. It is also found that the bias in the atomic charges due to the electrophilicity of the oxygen atom is strongly correlated with the induced dipole moment.

*Department of Chemistry, Graduate School of Science, Kyoto University, Sakyo-ku, Kyoto 606-8502, Japan.

INTRODUCTION

Hydrogen bond has been a topic of considerable interest due to its relevance in chemistry, biology and physics. In the field of materials science, the hydrogen-bonded organic and inorganic compounds exhibit various interesting transition phenomena, including ferroelectric and antiferroelectric phase transitions. The hydrogen bonding is involved in these transitions in forms of proton transfer, isotope effect and enhancement of the spontaneous electric polarization.[1,2]

5-bromo-9-hydroxyphenalenone ($C_{13}H_7O_2Br$; BHP) belongs to hydrogen-bonded dielectrics. Figure 1 shows the structure of BHP. This material has the intramolecular hydrogen bond ($O-H\cdots O$), and shows two successive phase transitions when H1 atom is substituted by a deuterium.[3]

From the structural analysis, it has been considered that BHP molecules in crystal are comparatively isolated from each other, *i.e.*, the so-called zero-dimensional hydrogen-bonded system. In previous work, however, we have shown that there exists $C-H\cdots O$ type intermolecular weak hydrogen bonding which notably affects the transition temperature through the enhancement of the molecular polarization.[4] These hydrogen bonds were found in two relative configurations as shown in Figures 2 and 3. As the evidence of the existence of the weak hydrogen bonding, we referred to the geometric feature (interatomic distances), the atomic charges obtained by the natural population analysis (NPA),[5] and the charge density in the $C-H\cdots O$ region calculated by using the density functional theory (DFT) with plane-wave basis sets.

In the present study, we extend the analysis by using Bader's theory of "Atoms in Molecules" (AIM)[6] in order to confirm and clarify the nature of the intermolecular hydrogen bonding. The AIM theory is based on the electron charge density ρ, and provides information about the nature of chemical bond and the bond strength. The usefulness of the AIM theory is well-documented: it has already been successfully applied to conventional hydrogen bonds, $C-H\cdots O$ bonds and $H\cdots H$ bonds (so-called dihydrogen bonds).[7–9] Koch and Popelier proposed a set of criteria to establish hydrogen bonding in $C-H\cdots O$ configurations.[7] In Table 1, we summarize the Koch-Popelier's eight criteria. The criteria (1)-(4)

are topological and local properties at bond critical point (BCP), which include the electron charge density at BCP (ρ_b) and the Laplacian of the electron charge density at BCP ($\nabla^2\rho_b$). The criteria (5)-(8), on the other hand, are the integrated properties of hydrogen atoms involved in the hydrogen bonding.

We assess the $C-H\cdots O$ interactions in the two configurations in Figures 2 and 3 against the list of criteria. As a result, it is shown that one fulfills all the criteria, which confirms the intermolecular hydrogen bond in the region. The other fulfills most of them but not all, which indicates that there exists an extremely weak hydrogen bonding. In addition, we have found BCPs in $Br\cdots H$ and $H\cdots H$ regions. The geometrical feature and topological feature obtained by the AIM analysis imply that the strength of these types of interactions is intermediate between the two $C-H\cdots O$ bonds mentioned above. The quantitative discussion is given about the correlation between the bias in the electron charge caused by the $C-H\cdots O$ bonds and the change of the molecular dipole moment induced by their neighboring molecules.

COMPUTATIONAL DETAILS

For the molecular and crystal geometry, we adopted the experimental data obtained by neutron diffraction at 10 K,[10] in order to correspond with our previous work.[4]

In the AIM analysis, we classified the neighboring molecules by their relative positions from one molecule. Because of the crystal symmetry, we can construct 13 types of trimers with the nearest neighboring molecules. As mentioned in Introduction, we focus on the two trimer configurations which have $C-H\cdots O$ contacts in the intermolecular region. We refer them as trimers I and II, which correspond to trimers I and F in our previous study,[4] respectively (See Figures 2 and 3).

Here, we define the position and direction of the molecules and atoms. First, all through the paper, we fix the central molecule of the trimers in the direction as can be seen in Figures 2 and 3. Then, we refer to the molecule in left (right) side of the central molecule as left (right) molecule. The H1 atom in the BHP molecule can attach to either of the two oxygen atoms. Thus, for each of the trimers, the AIM analysis is performed in all the four

cases corresponding to the positions of the two H1 atoms in surrounding molecules. (Note that it is sufficient to analyze with the H1 atom of the central molecule fixed to be one side, because of the crystal symmetry.) These four types of trimers are distinguished by the state of oxygen atoms of the surrounding molecules interacting with hydrogen atoms of the central molecule. For example, in case of trimer I (See Figure 2), when H1 of the left molecule is attached to the left (right) oxygen in the molecule, the carbonyl (enolic) oxygen interacts with H2 of the central molecule (H2‴ in Figure 2). Likewise, when H1 of the right molecule is attached to the left (right) oxygen in the molecule, the enolic (carbonyl) oxygen interacts with H2 of the central molecule (H2′ in Figure 2). Therefore, by using the indices C (carbonyl) and E (enolic) for interacting oxygen, we refer to the four trimers as CC, CE, EC, and EE: the first and second indices show the oxygen atoms in the left and right molecules, respectively. Both the trimers in Figures 2 and 3 correspond to the schematic structures of the trimer CE.

Calculations were performed at the HF/cc-pVDZ, HF/6-31++G(d,p) and B3LYP/6-31++G(d,p) levels with the program GAMESS,[11] and the resulting wave functions have been used to compute the topographical features of electron density using the AIMAll software package.[12]

RESULTS AND DISCUSSION

Assessment against the Koch-Popelier's criteria

In this section, we show the results obtained for the trimer CE, because there is no significant difference among the four trimers in each computational level: within 0.0004 au, 0.0006 au and 0.05 Å for ρ_b, $\nabla^2\rho_b$, and the position of BCP, respectively.

Topology

Figures 2 and 3 show the intermolecular arrangements of trimer I and II with BCPs marked by the small green points. As expected, the BCPs were found in the intramolecular $\mathrm{O-H\cdots O}$ and intermolecular $\mathrm{C-H\cdots O}$ regions. Furthermore, we can see that there exist BCPs in

the H$\cdots$H and Br$\cdots$H regions in trimer II. This indicates the accumulation of the electronic charge density in the intermolecular region, although the presence of BCP is not the sufficient condition for the existence of chemical bonding. Thus, the result of the AIM analysis implies the existence of four types of intermolecular bonds in trimer II: H3$\cdots$O, O$\cdots$H4, H4$\cdots$H2, and H2$\cdots$Br. Figure 3 shows that the O, H4, H2, and Br atoms can interact in a bifurcated manner.

In the following, we first assess the C$-$H$\cdots$O interactions against the other criteria. We state the possible consequences for other interactions in trimer II in a later subsection.

Electron densities and Laplacian of the electron density at the bond critical point

The electron density at the BCP ρ_b obtained at the HF/cc-pVDZ level is listed in Table 2. The values, 0.011 au for trimer I and 0.003 au for trimer II, obviously meet the criterion (2) and are consistent with our previous result of the intermolecular charge density for the corresponding trimers obtained by density functional theory with plane-wave basis set.[4] Since the electron density for trimer II is close to the lower limit of the criterion, we expect that this interaction is extremely weak. The indication for the weakness of the intermolecular interaction in trimer II is seen consistently in the following subsections.

The third criterion is about the Laplacian of the electron density, which designates the regions where the electronic charge is concentrated ($\nabla^2\rho < 0$), or locally depleted ($\nabla^2\rho > 0$). It is well known that $\nabla^2\rho_b$ is positive for hydrogen bonds, ionic bonds, and van der Waals interactions (so-called closed-shell interactions), while $\nabla^2\rho_b$ is negative for covalent bonds (shared interactions).[6,9] In Table 2, the values of Laplacian of the electron density at BCP $\nabla^2\rho_b$ are also shown. For trimer I, the values of $\nabla^2\rho_b$ fall within the range of the criterion (3). On the other hand, the values of $\nabla^2\rho_b$ for trimer II are positive, but smaller than the lower limit.

Table S1 in the Supplementary Material (SM) shows the topological parameters at the BCPs in the C$-$H$\cdots$O regions evaluated at the three computational levels. For all computational levels used in this study, we obtained practically the same values of each parameter, except for the ellipticity ϵ which is defined as $\epsilon = \lambda_1/\lambda_2 - 1$ (For ϵ and λ_j, see Appendix). From the definition, the value of ϵ is quite dependent on small relative changes in λ_1 and λ_2.

We shall not comment on the differences further in this work.

It is reported that the electron density and its Laplacian at BCP are almost independent of both the method and basis set.[13–15] Although it is mentioned that split-valence double-ζ type basis sets give worse results than split-valence triple-ζ type in Ref. 15, the differences between them are not so large as to affect the results discussed above.

Mutual penetration of hydrogen and acceptor atom

The mutual penetration is the quantity which describes how the hydrogen and acceptor atoms penetrate each other. In order to estimate the mutual penetration, the non-bonded radius and bonded radius for each atom need to be calculated. The non-bonded radius of an atom A, r_{A}^{0}, is defined as the distance from its nucleus to the electron density contour of 0.001 au in the monomer. This is measured in the direction to which intermolecular bonding is formed from the nucleus. The bonded radius r_{A} is defined here to be the distance between the nucleus and the intermolecular BCP in the trimer. The penetration Δr_{A} is expressed as

$$\Delta r_{\mathrm{A}} = r_{\mathrm{A}}^{0} - r_{\mathrm{A}}. \tag{1}$$

Table 3 shows the corresponding penetrations for the hydrogen and oxygen at the HF/cc-pVDZ level. As can be seen, all the penetration values calculated are positive, and the hydrogen atom is more penetrated than the oxygen atom. This feature has been reported for other $\mathrm{C-H\cdots O}$ type complexes.[7] In Table S2 in the SM we show the penetrations obtained at the three computational levels. The effect of the addition of diffuse functions appears in the non-bonded radii, which causes larger values of the mutual penetration.

Integrated properties of hydrogen atom

In this subsection, we discuss the criteria (5)-(8). In Table 4, we show the differences of the integrated properties for hydrogen atoms obtained at the HF/cc-pVDZ level. The differences are defined as the subtraction of the value in the isolated monomer from that in the trimers. Table S3 shows the integrated properties at the three computational levels. Henceforth in this subsection, we discuss the results evaluated at the HF/cc-pVDZ level. Although the

values are slightly different in each computational level, the discussion below applies in all the levels used.

The net charge on an atom q is given by the sum of the nuclear charge and the electronic charge of the atom. As is seen in Table 4, Δq is positive in all the hydrogen atoms in question. This result corresponds to a loss of electrons from the hydrogen atoms.

The sixth criterion is assessed with atomic energy destabilization ΔE, which is defined as the differences in atomic energy of the hydrogen between the trimers and the isolated monomer. The positive value means that the energy of hydrogen atom in the trimer is higher than that in the monomer. Note that the destabilization of the atom involved in closed-shell interaction often occurs but not necessarily: for example, it is reported that hydrogen atom is stabilized by forming an agostic bond ($\mathrm{C-H\cdots M; M = Metal}$).[16] It is thus worth assessing the change of the atomic energy as one of the criteria. The values of ΔE are shown in Table 4. We can see that the hydrogen atoms are destabilized in the trimers, although one small exception is found in trimer II.

The seventh criterion is assessed with the first moment $\mathbf{M}$, which is the atomic integration of a position vector times the electron density. Here, it is sufficient to consider its absolute value $|\mathbf{M}|$ in order to judge the criterion. From Table 4 it can be seen that the dipolar polarization is reduced in all the cases by constructing the trimers, which fulfills the criterion (7).

A final criterion is about the volume of the hydrogen atom v. In the AIM theory, the atomic volume is defined as the volume bounded by interatomic surfaces of the atom and an isosurface of the electron density of some chosen value. Here we take a value of 0.001 au for the contour. This contour encloses over 98 % of the electronic charges of each hydrogen atom. As can be seen in Table 4, all the hydrogen atoms in question do indeed shrink by 5.1-6.3 au and 0.7-2.4 au for trimer I and II, respectively.

Other intermolecular bonding

Here, we mention other types of interactions than $\mathrm{C-H\cdots O}$ interaction found in trimer II. The distances between the interacting atoms are shown in Table 5. These are closer to the corresponding sums of the van der Waals radii[17] (2.40 Å for $\mathrm{H\cdots H}$ and 3.05 Å for $\mathrm{Br\cdots H}$)

than the H···O distances (2.72 Å for H···O) in trimer II (See Table 2). Tables 5-7 (and S4-S6) show the results of the analysis for H···H and Br···H interactions. First, we assess the H···H interactions against the same criteria as those for C – H···O interactions shown in Table 1 according to Popelier.[8] Each value of ρ_b, $\nabla^2\rho_b$ and the mutual penetration is in the middle of each value for C – H···O interaction in trimer I and II; and the values of $\nabla^2\rho_b$ are almost the same as the lower limit of the criterion (3). The integrated properties of the hydrogen atoms shown in Table 7 and S6 meet the criteria (5)-(8) with some small exceptions of atomic energy. Therefore, according to both of the geometrical and topological view, it is considered that the strength of the interactions is intermediate between those of C – H···O interactions in trimers I and II. Recently, Echeverría *et al.* revealed that the attractive dihydrogen interactions between alkanes are stronger than usually thought with high-level (MP2, MP4 and CCSD(T)) methods.[18] Thus, the dihydrogen interactions in BHP can be analogously significant here, although it is difficult to evaluate the components of the bifurcated interactions separately.

It is reported that halogen atoms covalently bound to C atom are classified as weak hydrogen bond acceptors.[19] Judging from the value obtained by AIM analysis (See Tables 5, 6, S4 and S5), the strength of Br···H interactions are almost the same as that of the dihydrogen interactions.

Correlation between the induced molecular dipole moment and the bias in the atomic charge

In this section, we explain how the molecular dipole moment of BHP is induced by the neighboring molecules by using the atomic charges q. We define the change of the atomic charge for an atom A as

$$\Delta q(\mathrm{A}) = q_{\mathrm{tri}}(\mathrm{A}) - q_{\mathrm{mon}}(\mathrm{A}), \tag{2}$$

where $q_{\mathrm{tri}}(\mathrm{A})$ and $q_{\mathrm{mon}}(\mathrm{A})$ denote the atomic charge for an atom A in the central molecule of the trimer and that in the isolated monomer, respectively. The results at the HF/cc-pVDZ level are shown in Table 8. In this table, the values of Δq for atoms in the left and right sides from an axis through Cc1-Cc3 atoms (See Figure 1) are shown in each column separately.

Figure 4 shows the schematic plots of the results with the molecular structures. As can be seen, the charges of atoms which participate in the intermolecular bonding are mainly affected. In trimer I, Δq(H2) takes two values(~ 0.05 au or ~ 0.07 au), which depends on the oxygen atom interacting with the corresponding H2 atom. In the case of $\mathrm{H2}\cdots\mathrm{O_{car}}$ ($\mathrm{H2}\cdots\mathrm{O_{en}}$), Δq(H2) amounts to ~ 0.07 au (~ 0.05 au). Therefore we can attribute the difference in Δq(H2) to the difference between the electrophilicity of carbonyl oxygen and enolic oxygen. The same trend can be seen in trimer II, although the values of Δq(H3) and Δq(H4) are quite small reflecting the weakness of the interaction.

In order to analyze the correlation between Δq and the transverse dipole moment, we define the bias in the net charge in transverse direction $\Delta_{\mathrm{L-R}}$ as

$$\Delta_{\mathrm{L-R}} = \sum_{\mathrm{left}} \Delta q - \sum_{\mathrm{right}} \Delta q, \tag{3}$$

where the first and second terms are the sums of Δq's for atoms in the left and right sides from the central axis, respectively (except for H1 atom). The results are also shown in Table 8. In BHP, the transverse component of the molecular dipole moment points from the carbonyl oxygen to the enolic oxygen. Therefore, when $\Delta_{\mathrm{L-R}}$ is positive, the bias can lead to the enhancement of the transverse dipole moment. In the case where $\Delta_{\mathrm{L-R}}$ is negative, on the other hand, the bias induced by surrounding molecules can contribute to reduce the transverse component.

Note that $\Delta_{\mathrm{L-R}}$ most closely correlate with the difference between Δq of the left and right hydrogen atoms, which suggests that the bias is mainly due to the atomic charges of hydrogen induced by the oxygen atoms. It is also notable that the magnitude of $\Delta_{\mathrm{L-R}}$ in trimer II is close to that in trimer I. This indicates that the total contribution of the bifurcated $\mathrm{C-H}\cdots\mathrm{O}$ interaction is comparable to $\mathrm{C-H}\cdots\mathrm{O}$ interaction in trimer I, although each of $\mathrm{C-H}\cdots\mathrm{O}$ interaction in trimer II is quite weaker than that in trimer I. In Tables S7 and S8, we show the results at the level of HF/6-31++G(d,p) and B3LYP/6-31++G(d,p), respectively. Obviously the discussion presented above also applies in the results at these two levels.

Our present result is consistent with that of our previous study: the molecules in the positional relation of trimer II strongly affect the molecular dipole moment of BHP molecule

to the same degree as that of trimer I.[4] Figure 5 plots the relative change of the transverse dipole moment for central molecule in trimers I and II from that for isolated monomer $\Delta p_\perp$ against the bias $\Delta_{\mathrm{L-R}}$ both at the HF/cc-pVDZ level. The relative change $\Delta p_\perp$ is evaluated in the same manner as the previous work,[4] *i.e.*,

$$\Delta p_\perp = \left| \frac{p_\perp^{\mathrm{tri}}}{p_\perp^{\mathrm{mon}}} \right| - 1, \tag{4}$$

where $p_\perp^{\mathrm{mon}}$ is the transverse dipole moment of an isolated monomer and $p_\perp^{\mathrm{tri}}$ is that of the central molecule in a trimer. The dipole moment $p_\perp^{\mathrm{tri}}$ can be evaluated by using fragment molecular orbital (FMO) method[20]. We have calculated $p_\perp^{\mathrm{tri}}$ with the FMO method at the HF/cc-pVDZ level for all the four cases (CC, CE, EC, and EE) in each of trimer I and II. Here we show the result obtained at the HF/cc-pVDZ level only, because we have encountered the convergence problems in evaluating $p_\perp^{\mathrm{tri}}$ with the FMO method at the other computational levels.[21]

In Figure 5, we can see that there is a linear correlation between $\Delta p_\perp$ and $\Delta_{\mathrm{L-R}}$ (correlation coefficient 0.99). This strongly suggests that the bias in the atomic charge cause the enhancement of the molecular dipole moment in crystal, which contributes decisively to the transition temperature.[4] As mentioned above, the result of the AIM analysis suggests that H$\cdots$H and Br$\cdots$H interactions are not negligible, but they do not seem to contribute to the enhancement of the molecular polarization in the transverse direction.

CONCLUSIONS

In summary, we have investigated the intermolecular interactions of BHP by means of Bader's theory of Atoms in Molecules. In the AIM analysis, Koch-Popelier's criteria are applied in order to confirm the intermolecular C$-$H$\cdots$O hydrogen bonding. Although a few exceptions have been found, the two candidates for the C$-$H$\cdots$O bonding satisfy most of the criteria, which indicates the existence of the intermolecular hydrogen bonding: one is a normal type, and the other is a bifurcated one. In addition, other types of interactions, H$\cdots$H and Br$\cdots$H, have been found. The geometrical and topological parameters indicate that the strength of these interactions is intermediate between the two C$-$H$\cdots$O bonding.

The bias in the atomic charge is also evaluated. Our results show that the bias is mainly caused by the difference of electrophilicity between carbonyl and enolic oxygen involved in the $C-H\cdots O$ bonding. It is also found that the bias is strongly correlated with the induced dipole moment which determines the transition temperature of dielectric phase transition. Each of the $C-H\cdots O$ interactions in the bifurcated bonding is quite weak, but the total contribution to the dipole induction is comparable with the typical $C-H\cdots O$ bond.

ACKNOWLEDGMENTS

The authors acknowledge the support by the Global COE Program "International Center for Integrated Research and Advanced Education in Materials Science" of the Ministry of Education, Culture, Sports, Science and Technology (MEXT) of Japan. KA acknowledges supports from KAKENHI Nos. 20108017 ("π-space") and 22550012.

APPENDIX

In this appendix, we briefly summarize the BCP properties referred in the present work. The BCP is one of the critical points (CPs), which are defined as the points where $\nabla\rho$ vanishes. The CPs are classified by the curvatures at their own positions. Mathematically, they correspond to the three eigenvalues λ_j ($j=1,2,3; \lambda_1<\lambda_2<\lambda_3$) of the Hessian of ρ. The BCP is characterized by one positive and two negative curvatures of ρ, *i.e.*, $\lambda_1<\lambda_2<0<\lambda_3$. In Tables 2 and 5 (See also Tables S1 and S4), we can confirm numerically that all the intermolecular CPs in the BHP trimer configurations are BCPs.

Two quantities used in the AIM analysis are expressed by using λ_j: one is the Laplacian of the electron density $\nabla^2\rho_b=\sum_{j=1}^{3}\lambda_j$ and the other is the ellipticity $\epsilon=\lambda_1/\lambda_2-1$. The Laplacian $\nabla^2\rho_b$ is involved in the Koch-Popelier's criteria (See Table 1) and has already been discussed. The ellipticity provides a measurement of the anisotropy of the electron density and reflects structural instability.[22] The result of ϵ shown in Tables 2 and 5 (See also Tables S1 and S4) implies that the $C-H3\cdots O$ bond is much more stable than the $C-H4\cdots O$ bond in trimer II, and the stability of the $H\cdots H$ and $Br\cdots H$ bonds in trimer

II is roughly the same order as that of $C-H4\cdots O$ bond in trimer II. The values of ϵ for $C-H3\cdots O$ bonds in trimer II are the same order as those for $C-H2\cdots O$ bonds in trimer I. However, judging from the other quantities discussed above, it is difficult to conclude that these bonds have similar stability.

References

1. S. Horiuchi and Y. Tokura, Nat. Mater. **7**, 357 (2008)

2. S. Horiuchi, F. Ishii, R. Kumai, Y. Okimoto, H. Tachibana, N. Nagaosa, and Y. Tokura, Nat. Mater. **4**, 163 (2005)

3. T. Mochida, A. Izuoka, T. Sugawara, Y. Moritomo, and Y. Tokura, J. Chem. Phys. **101**, 7971 (1994)

4. H. Otaki and K. Ando, Phys. Chem. Chem. Phys. **13**, 10719 (2011)

5. A. E. Reed, L. A. Curtiss, and F. Weinhold, Chem. Rev. **88**, 899 (1988)

6. R. F. W. Bader, *Atoms in Molecules: A Quantum Theory* (Clarendon, Oxford, 1990)

7. U. Koch and P. L. A. Popelier, J. Phys. Chem. **99**, 9747 (1995)

8. P. L. A. Popelier, J. Phys. Chem. A **102**, 1873 (1998)

9. S. J. Grabowski, *Hydrogen Bonding - New Insights*, Challenges and Advances in Computational Chemistry and Physics, Vol. 3 (Springer, 2006)

10. R. Kiyanagi, H. Kimura, M. Watanabe, Y. Noda, T. Mochida, and T. Sugawara, J. Phys. Soc. Jpn. **77**, 064602 (2008)

11. M. W. Schmidt, K. K. Baldridge, J. A. Boatz, S. T. Elbert, M. S. Gordon, J. H. Jensen, S. Koseki, N. Matsunaga, K. A. Nguyen, S. Su, T. L. Windus, M. Dupuis, and J. A. Montgomery, J. Comput. Chem. **14**, 1347 (1993)

12. T. A. Keith, "AIMAll (version 11.09.18)," aim.tkgristmill.com (2011)

13. K. B. Wiberg and P. R. Rablen, J. Comput. Chem. **14**, 1504 (1993)

14. C. F. Matta, J. Comput. Chem. **31**, 1297 (2010)

15. M. Jabłoński and M. Palusiak, J. Phys. Chem. A **114**, 2240 (2010)

16. P. L. A. Popelier and G. Logothetis, J. Organomet. Chem. **555**, 101 (1998)

17. A. Bondi, J. Phys. Chem. **68**, 441 (1964)

18. J. Echeverría, G. Aullón, D. Danovich, S. Shaik, and S. Alvarez, Nat. Chem. **3**, 323 (2011)

19. G. R. Desiraju and T. Steiner, *The Weak Hydrogen Bond* (Oxford University Press, New York, 2001)

20. K. Kitaura, E. Ikeo, T. Asada, T. Nakano, and M. Uebayasi, Chem. Phys. Lett. **313**, 701 (1999)

21. E. B. Starikov, J. P. Lewis, and S. Tanaka, *Modern Methods for Theoretical Physical Chemistry of Biopolymers* (Elsevier, Amsterdam, 2006)

22. D. Cremer, E. Kraka, T. S. Slee, R. F. W. Bader, C. D. H. Lau, T. T. Nguyen-Dang, and P. J. MacDougall, J. Am. Chem. Soc. **105**, 5069 (1983)

23. K. Momma and F. Izumi, J. Appl. Crystallogr. **41**, 653 (2008)

Figure 1: Structure of BHP molecule. Atomic labels are also shown. The two oxygen atoms, O_{en} and O_{car}, denote an enolic oxygen and a carbonyl oxygen, respectively. The software VESTA[23] was used for the drawing.

Figure 2: Intermolecular arrangement of BHP trimer I. Small (green) points on the bonds mark the bond critical points.

Figure 3: Intermolecular arrangement of BHP trimer II. Small (green) points on the bonds mark the bond critical points.

Figure 4: Difference of the atomic charges between the monomer and the central molecule of (a) trimer I and (b) trimer II both evaluated at the HF/cc-pVDZ level. The magnitude of the positive (negative) value is proportional to the area of the red (blue) circle.

Figure 5: Correlation between Δ_{L-R} and $\Delta p_{\perp}$ obtained at the HF/cc-pVDZ level.

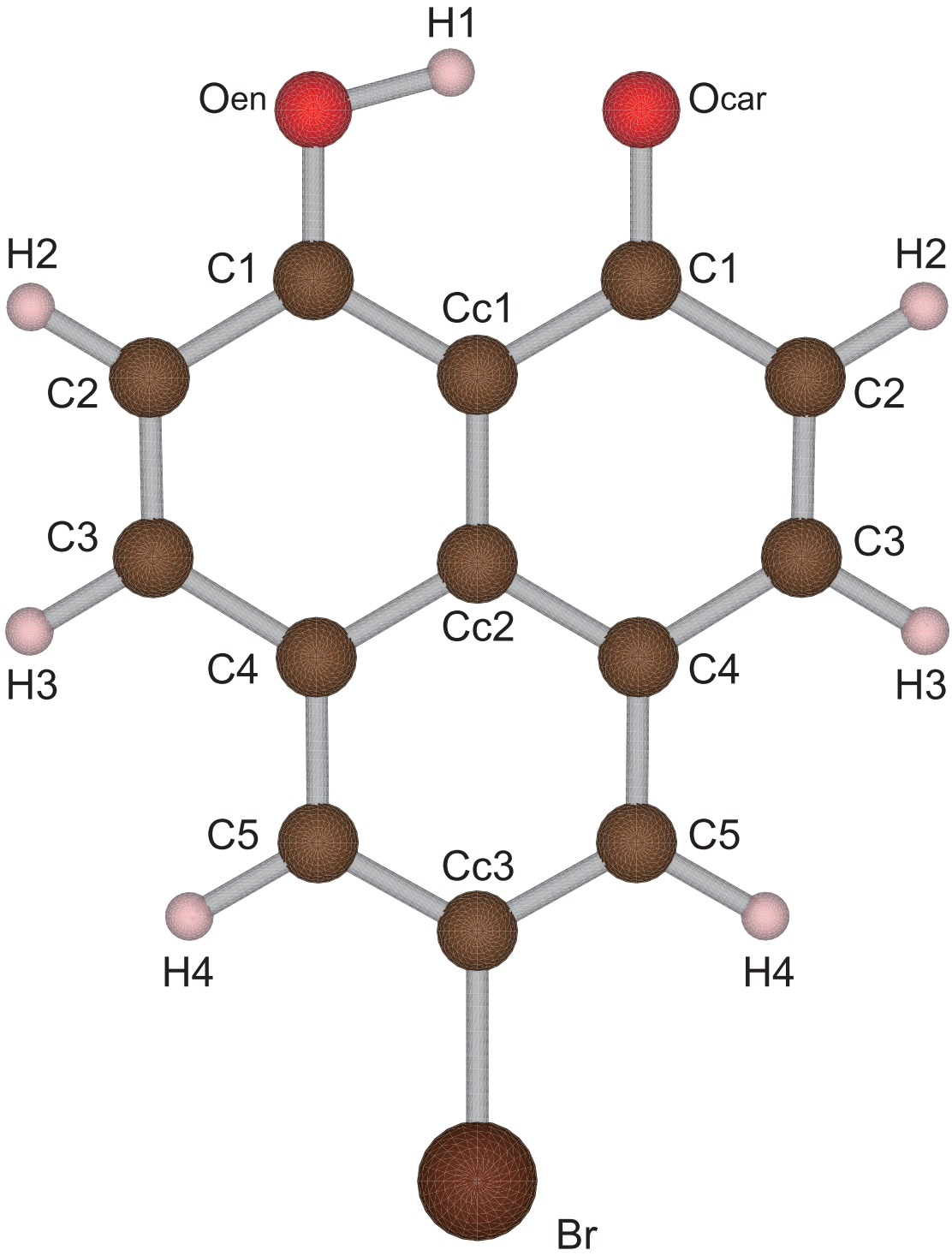

Figure 1
Hiroki Otaki, Koji Ando
Int. J. Quant. Chem.

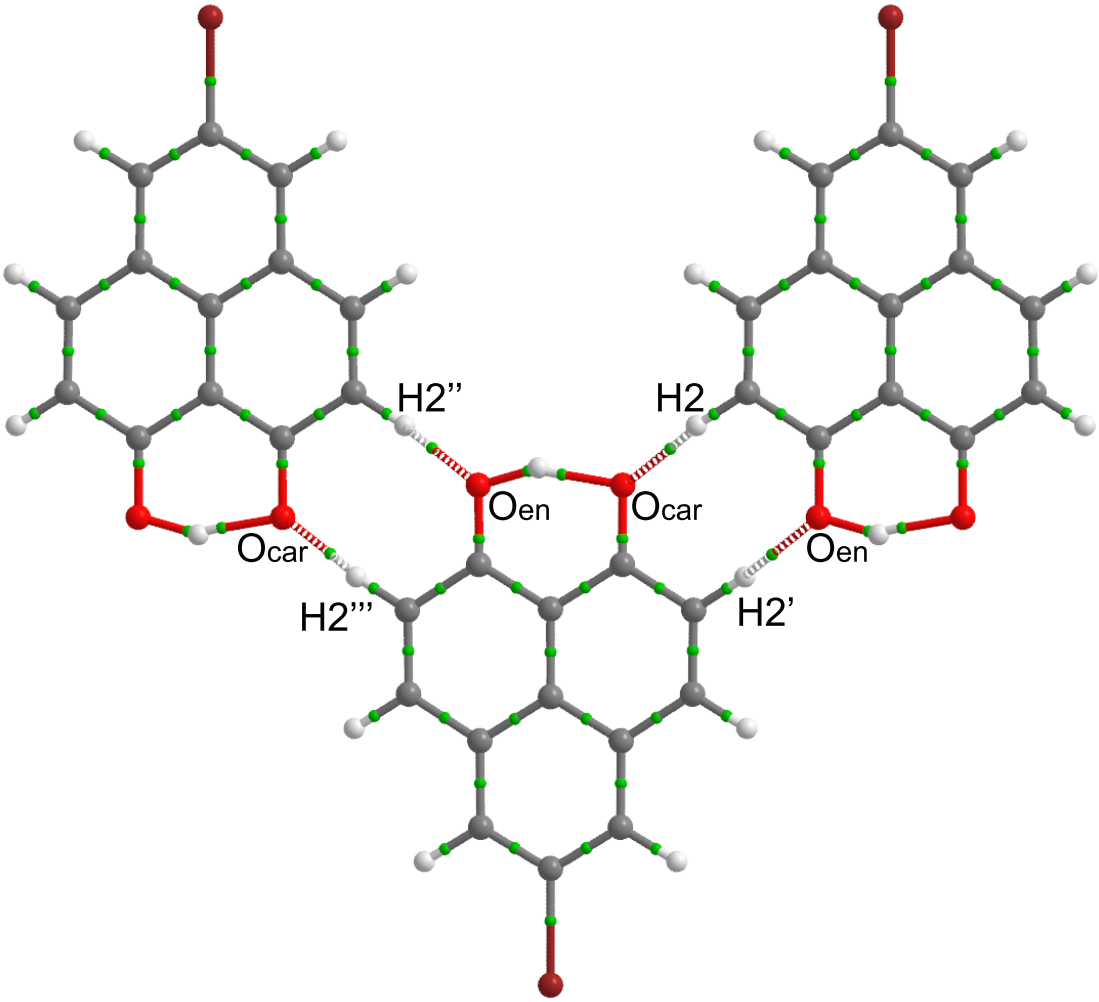

Figure 2
Hiroki Otaki, Koji Ando
Int. J. Quant. Chem.

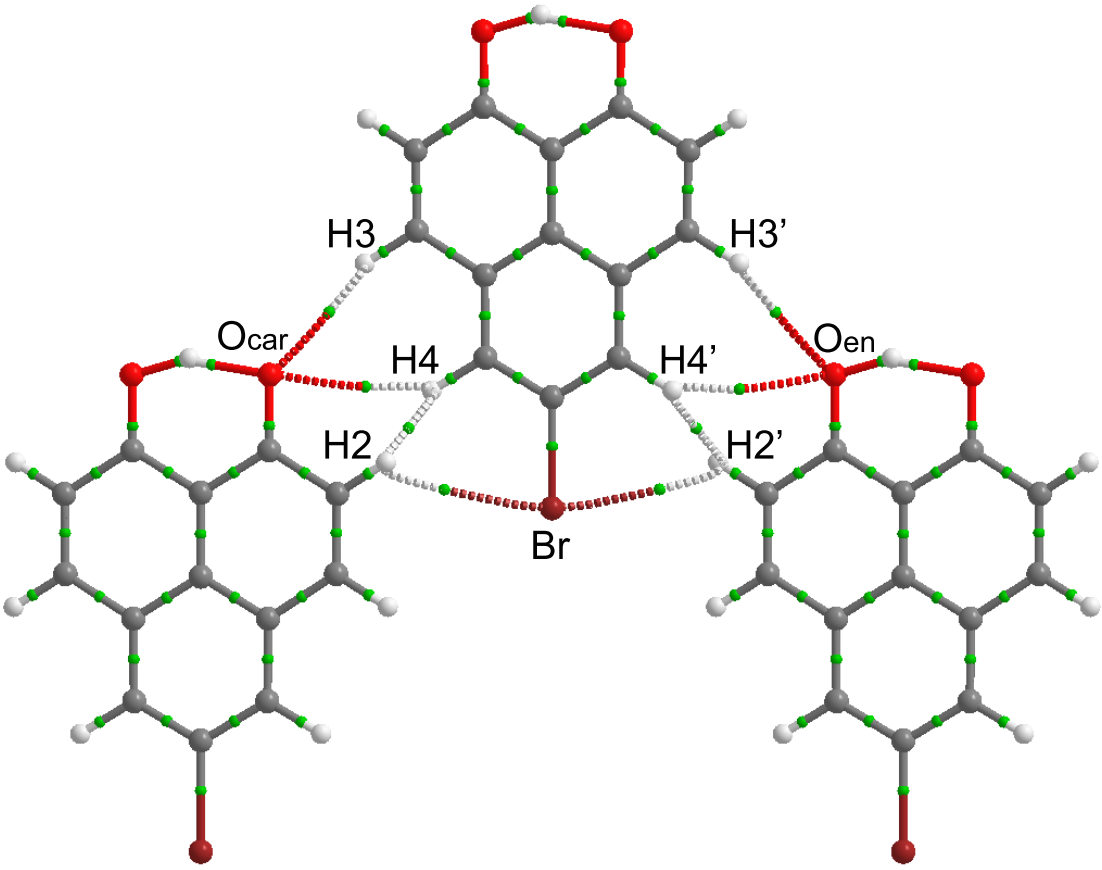

Figure 3
Hiroki Otaki, Koji Ando
Int. J. Quant. Chem.

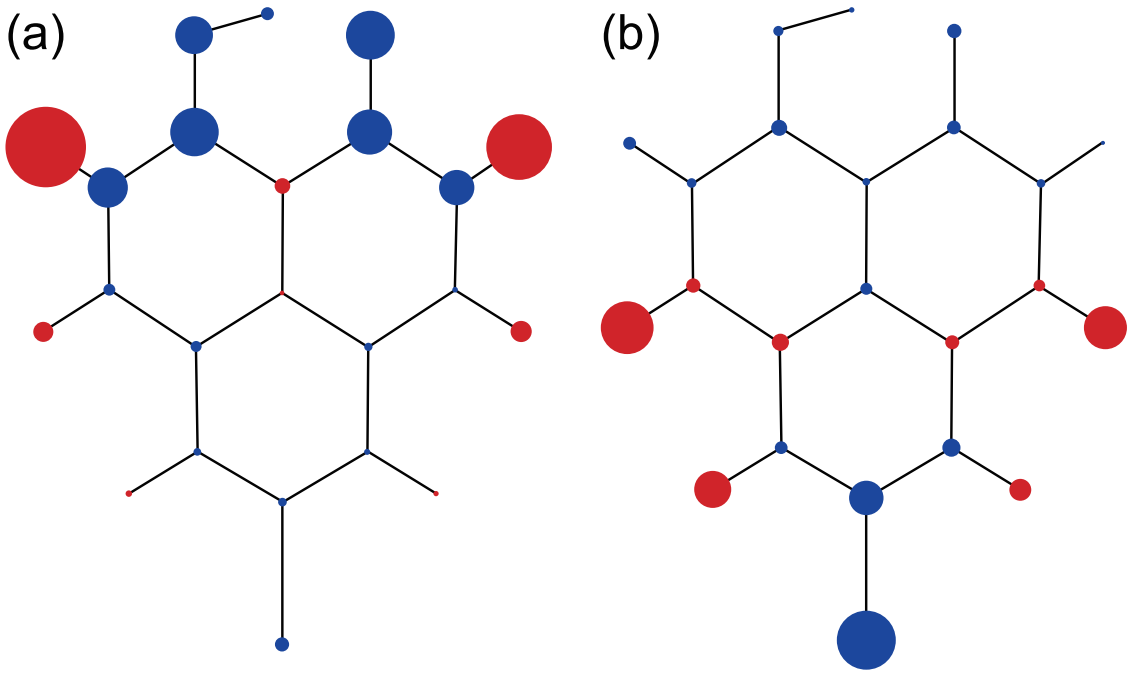

Figure 4
Hiroki Otaki, Koji Ando
Int. J. Quant. Chem.

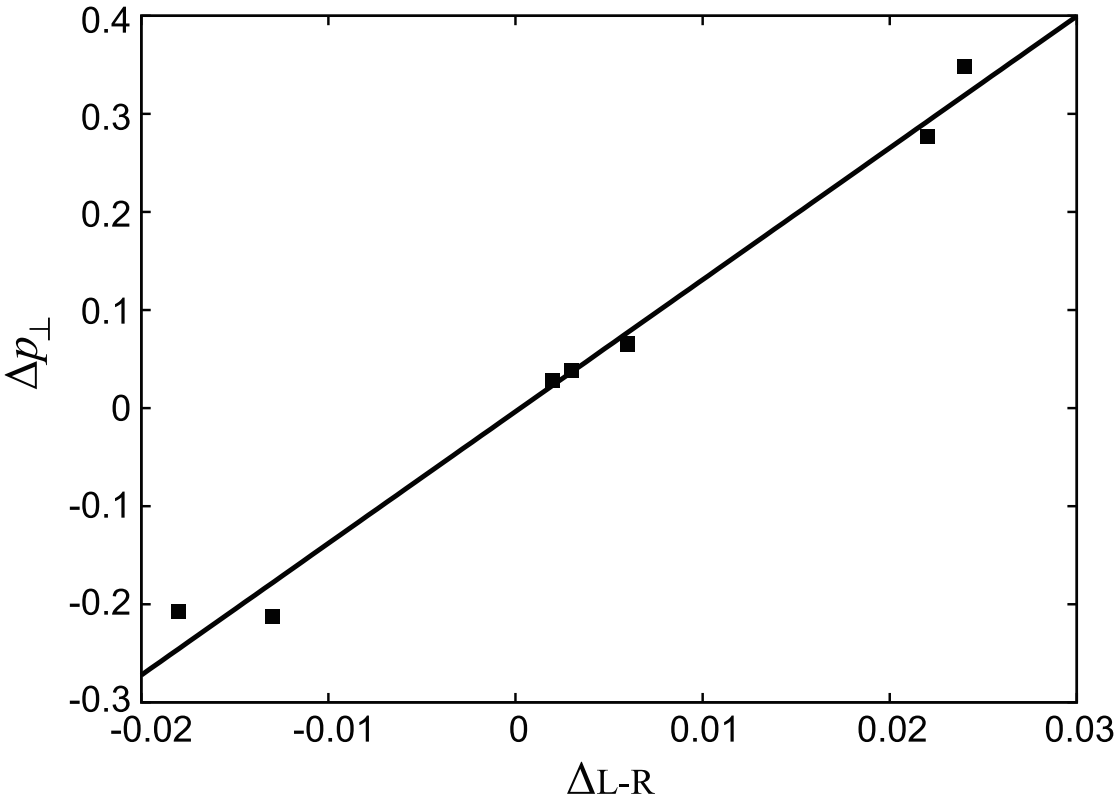

Figure 5
Hiroki Otaki, Koji Ando
Int. J. Quant. Chem.

(1)	Topology: a BCP for a hydrogen bond must be topologically found
(2)	Proper value of electron density at the BCP ($0.002 - 0.035$ au)
(3)	Proper value of Laplacian of electron density at the BCP ($0.024 - 0.139$ au)
(4)	Mutual penetration: the hydrogen and the acceptor atoms penetrate each other
(5)	Increase of net charge of the hydrogen atom
(6)	Energetic destabilization of the hydrogen atom
(7)	Decrease in dipolar polarization of the hydrogen atom
(8)	Decrease in atomic volume of the hydrogen atom

Table 1: Koch-Popelier's eight criteria for C–H$\cdots$O hydrogen bond

Trimer	BCP	d	ρ_b	$\nabla^2\rho_b$	λ_1	λ_2	λ_3	ϵ
I	$O_{car}\cdots H2(H2''')$	2.39	0.011	0.035	-0.012	-0.011	0.058	0.078
	$O_{en}\cdots H2'(H2'')$	2.39	0.011	0.035	-0.012	-0.011	0.058	0.089
II	$O_{car}\cdots H3$	2.95	0.003	0.015	-0.003	-0.003	0.020	0.092
	$O_{en}\cdots H3'$	2.95	0.003	0.015	-0.003	-0.003	0.020	0.075
	$O_{car}\cdots H4$	3.01	0.003	0.015	-0.002	-0.001	0.019	1.048
	$O_{en}\cdots H4'$	3.01	0.003	0.015	-0.002	-0.000^a	0.017	4.899

[a]The value is negative and its absolute value is less than 0.001.

Table 2: Interatomic distances d (in Å) and BCP properties (in au) of the analyzed trimers for C–H$\cdots$O interactions evaluated at the HF/cc-pVDZ level. For $\lambda_j (j = 1, 2, 3)$ and ϵ, see Appendix

Trimer	O ⋯ H	r_{O}^{0}	r_{O}	Δr_{O}	r_{H}^{0}	r_{H}	Δr_{H}	$\Delta r_{\mathrm{H}} + \Delta r_{\mathrm{O}}$
I	$\mathrm{O_{car}} \cdots \mathrm{H2(H2'''')}$	1.77	1.46	0.31	1.33	0.93	0.40	0.71
	$\mathrm{O_{en}} \cdots \mathrm{H2'(H2'')}$	1.76	1.45	0.31	1.33	0.94	0.39	0.70
II	$\mathrm{O_{car}} \cdots \mathrm{H3}$	1.74	1.70	0.04	1.38	1.26	0.12	0.16
	$\mathrm{O_{en}} \cdots \mathrm{H3'}$	1.74	1.70	0.04	1.39	1.26	0.13	0.17
	$\mathrm{O_{car}} \cdots \mathrm{H4}$	1.83	1.74	0.09	1.38	1.27	0.11	0.20
	$\mathrm{O_{en}} \cdots \mathrm{H4'}$	1.80	1.73	0.07	1.38	1.29	0.09	0.16

Table 3: Bonded and non-bonded radii and mutual penetration for C–H$\cdots$O interactions obtained at the HF/cc-pVDZ level (in Å)

Trimer	Atom	Δq	ΔE	$\Delta\lvert\mathbf{M}\rvert$	Δv
I	H2	0.073	0.030	−0.011	−6.28
	H2′	0.047	0.016	−0.016	−5.13
	H2″	0.050	0.018	−0.016	−5.24
	H2‴	0.070	0.028	−0.011	−6.17
II	H3	0.030	0.012	−0.003	−1.17
	H3′	0.020	0.008	−0.004	−0.74
	H4	0.015	0.004	−0.006	−2.41
	H4′	0.005	−0.001	−0.007	−1.96

Table 4: Differences in the integrated properties of the hydrogen atoms between the trimers and the isolated monomer obtained at the HF/cc-pVDZ level (in au)

Trimer	BCP	d	ρ_b	$\nabla^2\rho_b$	λ_1	λ_2	λ_3	ϵ
II	$\mathrm{H4} \cdots \mathrm{H2}$	2.46	0.006	0.024	−0.005	−0.003	0.031	0.865
	$\mathrm{H4'} \cdots \mathrm{H2'}$	2.46	0.006	0.024	−0.005	−0.003	0.031	0.903
	$\mathrm{Br} \cdots \mathrm{H2}$	3.18	0.005	0.018	−0.004	−0.002	0.024	0.567
	$\mathrm{Br} \cdots \mathrm{H2'}$	3.18	0.005	0.018	−0.004	−0.002	0.024	0.535

Table 5: Interatomic distances d (in Å) and BCP properties (in au) for other intermolecular interactions evaluated at the HF/cc-pVDZ level. For $\lambda_j (j = 1, 2, 3)$ and ϵ, see Appendix

Trimer	A $\cdots$ B	r_{A}^{0}	r_{A}	Δr_{A}	r_{B}^{0}	r_{B}	Δr_{B}	$\Delta r_{\mathrm{A}} + \Delta r_{\mathrm{B}}$
II	H4$\cdots$H2	1.47	1.21	0.26	1.50	1.25	0.25	0.51
	H4$'\cdots$H2$'$	1.47	1.21	0.26	1.49	1.25	0.24	0.50
	Br$\cdots$H2	2.26	1.96	0.30	1.41	1.25	0.16	0.45
	Br$\cdots$H2$'$	2.26	1.96	0.30	1.41	1.25	0.16	0.46

Table 6: Bonded and non-bonded radii and mutual penetration for other interactions obtained at the HF/cc-pVDZ level (in Å)

Trimer	Atom	Δq	ΔE	$\Delta\lvert\mathbf{M}\rvert$	Δv
II	H2	0.006	0.000	-0.007	-2.10
	H2$'$	0.008	0.001	-0.006	-2.16
	H4	0.015	0.004	-0.006	-2.41
	H4$'$	0.005	-0.001	-0.007	-1.96

Table 7: Differences in the integrated properties of the hydrogen atoms between the trimers and the isolated monomer for other interactions obtained at the HF/cc-pVDZ level (in au)

Trimer	Atom	CE		CC		EE		EC	
		Left	Right	Left	Right	Left	Right	Left	Right
I	O	-0.015	-0.026	-0.016	-0.025	-0.016	-0.025	-0.017	-0.024
	C1	-0.025	-0.022	-0.026	-0.023	-0.025	-0.021	-0.026	-0.022
	C2	-0.017	-0.013	-0.018	-0.018	-0.013	-0.013	-0.013	-0.017
	H2	0.070	0.047	0.068	0.067	0.050	0.048	0.048	0.069
	$\sum \Delta q$	0.013	-0.011	0.005	0.000	0.002	-0.003	-0.005	0.007
	$\Delta_{\mathrm{L-R}}$	0.024		0.006		0.006		-0.013	
II	H3	0.030	0.020	0.029	0.028	0.022	0.021	0.020	0.030
	H4	0.015	0.005	0.013	0.013	0.007	0.007	0.006	0.014
	$\sum \Delta q$	0.042	0.020	0.034	0.031	0.030	0.029	0.022	0.040
	$\Delta_{\mathrm{L-R}}$	0.022		0.003		0.002		-0.018	

Table 8: Difference of the atomic charges Δq at the HF/cc-pVDZ level (in au). The values are shown whose absolute values are over 0.01 au and 0.005 au in trimer I and II, respectively